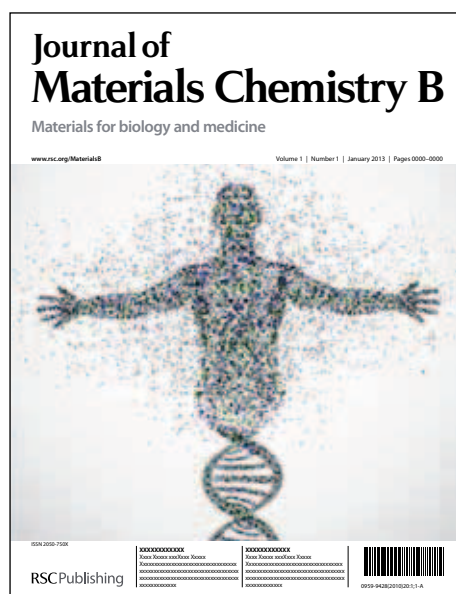


# Journal of Materials Chemistry B

Accepted Manuscript



This is an *Accepted Manuscript*, which has been through the RSC Publishing peer review process and has been accepted for publication.

*Accepted Manuscripts* are published online shortly after acceptance, which is prior to technical editing, formatting and proof reading. This free service from RSC Publishing allows authors to make their results available to the community, in citable form, before publication of the edited article. This *Accepted Manuscript* will be replaced by the edited and formatted *Advance Article* as soon as this is available.

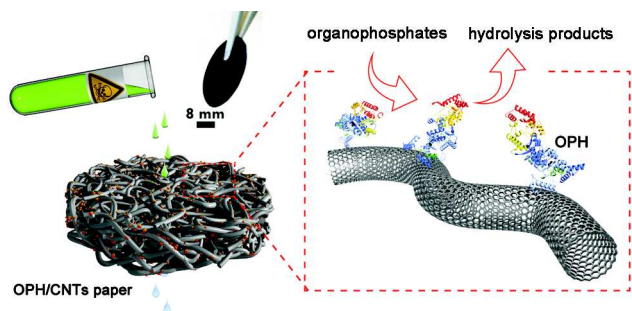
To cite this manuscript please use its permanent Digital Object Identifier (DOI®), which is identical for all formats of publication.

More information about *Accepted Manuscripts* can be found in the [Information for Authors](#).

Please note that technical editing may introduce minor changes to the text and/or graphics contained in the manuscript submitted by the author(s) which may alter content, and that the standard [Terms & Conditions](#) and the [ethical guidelines](#) that apply to the journal are still applicable. In no event shall the RSC be held responsible for any errors or omissions in these *Accepted Manuscript* manuscripts or any consequences arising from the use of any information contained in them.

## Table of contents

This work presents a new ‘one-pot’ generic methodology for a rapid and straightforward fabrication of enzymatically-active carbon nanotubes (CNTs) paper for organophosphates bioremediation. The enzyme organophosphate hydrolase (OPH) is immobilized onto CNTs simultaneously to membrane formation process.



## ARTICLE

# Biocatalytic carbon nanotube paper: 'One-pot' route for fabrication of enzyme-immobilized membranes for organophosphates bioremediation

Cite this: DOI: 10.1039/x0xx00000x

Received 00th January 2012,  
Accepted 00th January 2012

DOI: 10.1039/x0xx00000x

[www.rsc.org/](http://www.rsc.org/)Guy Mechrez<sup>a</sup>, Maksym A. Krepker<sup>b</sup>, Yifat Harel<sup>c</sup>, Jean-Paul Lellouche<sup>c</sup>, and Ester Segal<sup>b,†\*</sup>

Recent world events have demonstrated the critical need for facile and miniaturized bioremediation technologies of organophosphates (OPs). These compounds are among the most toxic substances synthesized to date and are used as pesticides and nerve agents. Biotechnological methods based on the use of organophosphate hydrolase (OPH) for detoxification of OPs have drawn significant attention. This work presents a new 'one-pot' methodology for a rapid and straightforward fabrication of enzymatically-active carbon nanotubes (CNT) paper for OPs bioremediation. Carboxylated CNTs are ultrasonically dispersed in an aqueous surfactant solution followed by a microfiltration process, to generate a paper-like membrane, which is assembled from entangled nanotubes. Herein, OPH conjugation to the CNTs is carried out by carbodiimide chemistry during the microfiltration process. Successful covalent immobilization of the enzyme onto the nanotubes surface is confirmed by cryo-transmission electron microscopy and infrared spectroscopy. To study the potential of this platform for OPs bioremediation, an aqueous solution of methyl paraoxon (used as a model OP) is filtered by the resulting OPH-CNT membranes. Significant decrease of methyl paraoxon concentration is obtained, ascribed to its in situ hydrolysis by the immobilized OPH during the filtration process. These thin membranes allow performing many subsequent filtration cycles, while maintaining their enzymatic activity, owing to the unique combination of mechanically robust CNT scaffold and high OPH loading. This study presents a new generic approach for the design of bioactive paper-like scaffolds, which can be rationally tailored for a variety of applications.

## 1. Introduction

Organophosphates (OPs) are potent inhibitors of the enzyme acetylcholinesterase (AChE) and their acute toxicity is attributed to the excessive cholinergic stimulation caused by inhibition of this enzyme at the neuromuscular junctions and in the central nervous system<sup>1,2</sup>. Synthetic OPs are widely used in agriculture and also as chemical warfare agents<sup>3,4,5</sup>. The World Health Organization reports on three millions cases of OPs-related poisonings worldwide<sup>2</sup>, mainly due to the accumulation of these toxic compounds in ground and surface waters<sup>6</sup>. Therefore, numerous methods for OPs removal and detoxification have emerged<sup>7-17</sup>, including oxidation<sup>7,8</sup>, reverse osmosis<sup>13</sup>, activated carbon adsorption<sup>12</sup>, and biodegradation<sup>18</sup>. Specifically, biotechnological methods for

OPs detoxification, involving the enzyme organophosphate hydrolase (OPH), have drawn significant attention<sup>19,20</sup>.

OPH is a ~35 kDa enzyme, characterized by very high affinity towards OPs, capable of their reversible binding and subsequent hydrolysis<sup>21,22,23,24</sup>. Detoxification of OPs by OPH requires a stable, highly efficient, and cost-effective system. The immobilization of OPH on a given scaffold may meet these demands, and provide the means whereby toxic substances can be efficiently degraded in a continuous process<sup>25</sup>. Immobilization of OPH onto different types of scaffolds<sup>25</sup>, including cellulose<sup>19</sup>, trityl agarose<sup>26</sup> and amyloid fibrils<sup>18</sup>, have been investigated for the development of bioremediation systems.

Over the past decade carbon nanotubes (CNT) have attracted significant attention for enzyme immobilization owing to their large surface area, chemical inertness, superior

## ARTICLE

mechanical properties and electrical conductivity<sup>5, 27-31</sup>. Specifically, CNT paper, which is a paper-like CNT film<sup>32-38</sup> (also termed as buckypaper) has recently emerged as promising scaffolds for enzyme immobilization with exciting potential applications as enzyme-based biofuel cells<sup>39-41</sup> and biosensors<sup>42</sup>. However, to date, CNT papers have not been studied for enzyme-immobilized biocatalytic membranes, despite the numerous publications focusing on buckypaper for conventional membrane technology<sup>33, 43-46</sup>.

This work presents a new 'one-pot' methodology for the fabrication of an enzymatically-active CNT paper for OPs bioremediation. Based on a preliminary study on the enzymatic activity of different OPH-CNT conjugates, an 'in-house' synthesized carboxylated multi-walled CNTs (MWNTs) are identified to exhibit superior catalytic activity. Thus, these carboxylated MWNTs are further used for the construction of OPH-immobilized CNT paper. The COOH-MWNTs are ultrasonically dispersed in an aqueous surfactant solution followed by a microfiltration process, to generate a thin paper-like membrane. *In situ* OPH conjugation is carried out by carbodiimide chemistry during CNT paper formation process. The covalent attachment of the OPH to the MWNTs surface is confirmed. To demonstrate the potential of the resulting OPH-CNT papers for bioremediation, we have studied the effect of treating a model OP (methyl paraoxon, MOX) solution with these miniaturized membranes. Significant decrease in MOX concentration is obtained, which is ascribed to its *in situ* hydrolysis by the immobilized OPH during the filtration process. Thus, this generic process allows for a rapid and facile construction of enzymatically-active nanostructured scaffolds for a variety of applications.

## 2. Experimental section

### 2.1 Materials and buffers

Both types of MWNTs, *i.e.*, NC 7000 (Nanocyl, Belgium) and NanoAmor (Amorphous Materials, Inc., USA) have been chemically oxidized. Commercially available oxidized MWCNTs (COOH-MWCNTs), *i.e.*, TNMC3 (Timesnano, China), COOH-DWNTs, and NC 2101 (Nanocyl, Belgium) were used as received without further purification. The surfactant Triton X-100, 1-Ethyl-3-(3-dimethylaminopropyl) carbodiimide hydrochloride (EDC), N-Hydroxysuccinimide (NHS), and methyl paraoxon (MOX) were obtained from Sigma Aldrich Chemicals. Organophosphorus hydrolase (OPH, EC 3.1.8.1) was supplied by Lybradyn, Inc. Oak Brook, IL, USA. All materials were used as received without further purification. 2-(4-Morpholino)ethanesulfonic acid (MES) (Sigma Aldrich Chemicals) buffer 0.5 M was prepared by dissolving the appropriate amount of MES in double distilled water. The pH of the buffer was adjusted to 6.1 with a necessary amount of 0.1 M NaOH (Frutarom, Israel). Phosphate buffered saline (PBS) pH 7.4 was prepared by dissolving di-sodium hydrogen phosphate anhydrous (Carlo Erba Reagenti) and dihydrogen orthophosphate anhydrous (Loba Chemie PVT Ltd.) in double distilled water at a predetermined ratio to yield the proper pH value. 2-(Cyclohexylamino)ethanesulfonic acid (CHES) (Sigma Aldrich Chemicals) buffer 0.02 M was prepared by dissolving the appropriate amount of MES in in double distilled water. The pH of the buffer was adjusted to 9 with an appropriate amount of 0.1M NaOH (Frutarom). 5% v/v of methanol (Gadot Ltd)

and 0.01 M of CoCl<sub>2</sub> (Sigma Aldrich Chemicals) were added to the CHES buffer.

### 2.2 Synthesis of COOH-MWNTs

Carboxylated MWNTs (COOH-MWNTs) were prepared according to a previously reported oxidative wet-chemistry method<sup>26, 47, 48</sup>, *i.e.*, the use of an oxidative acidic 1/1 v/v mixture of concentrated 12 M HNO<sub>3</sub> and 36 M H<sub>2</sub>SO<sub>4</sub> (90°C, 1.5 h) followed by multiple rinsing with double-distilled water until neutrality. The process results in the carboxylative opening of oxidation-sensitive end-caps, and in the introduction of defect carboxylic (COOH) groups on sidewall surfaces of oxidized COOH-MWNTs.

### 2.3 Synthesis of OPH/COOH-CNTs conjugates

COOH-CNTs (140 mg) were dispersed an aqueous Triton X-100 solution (200 mL) by ultrasonication (Vibra cell VCX 750 - Sonics & Materials Inc., USA). The MWNT:Triton X-100 weight ratio was kept constant at 1:5 in all samples. Ultrasonication was performed at a temperature of 4°C for 15 min at amplitude of 10% to form uniform COOH-CNTs dispersions. The resulting dispersions were mixed with 0.1 mL of MES buffer (0.5 M pH 6.1) and NHS (0.23 mL of 25 mg/mL). Subsequently, 0.12 mL of aqueous EDC solution (5 mg/mL) was added to the dispersion and gently stirred for 30 min. The resulting dispersions were centrifuged at 13,000 rpm for 6 min and the CNTs sediment was re-dispersed in 0.9 mL PBS. Centrifugation and re-dispersion steps were carried out 3 times. 0.1 mL solution of OPH in PBS at a concentration of 1 mg/mL was added to the re-dispersed COOH-CNTs and allowed to react at 4°C for 15 h under agitation. To separate the OPH/COOH-CNTs conjugates from any unreacted species, centrifugation at 13,000 rpm for 6 min was carried out and the sedimented conjugates were re-dispersed in 0.94 mL of CHES buffer. The centrifugation and re-dispersion steps were repeated 3 times.

### 2.4 Enzymatic activity measurement of immobilized OPH

As a model OP solution, MOX was dissolved in CHES buffer to a concentration of 25 mM. 60 µL aliquots of this solution were added to the aforementioned different OPH/COOH-CNTs dispersions and incubated at room temperature for 5 h. The catalytic activity of the immobilized OPH on CNTs was determined spectrophotometrically by monitoring p-nitrophenol formation during MOX hydrolysis. At specified time points, aliquots (150 µL) were sampled and centrifuged at 13,000 rpm for 3 min. The supernatant (100 µL) was mixed with an equivalent volume of CHES buffer and p-nitrophenol was monitored by absorbance measurements at 347 nm using a microplate reader (Varioskan Flash, Thermo Scientific, USA).

### 2.4 'One-pot' fabrication of OPH/COOH-MWNTs papers

COOH-MWNTs (140 mg) were dispersed an aqueous Triton X-100 solution (200 mL) by ultrasonication (Vibra cell VCX 750 - Sonics & Materials Inc., USA). The MWNT:Triton X-100 weight ratio was kept constant at 1:5 in all samples. Ultrasonication was performed at a temperature of 4°C for 15 min at amplitude of 10% to form uniform COOH-CNTs dispersions. 14.5 mL of the COOH- MWNTs dispersion was mixed with 1.5 mL of PBS, EDC solution in 0.05M PBS (1.5 mL of 20 mg/mL), and OPH solution in 0.05M PBS (4 mL of 5 mg/mL). The resulting mixture was immediately filtered

through a 0.45  $\mu\text{m}$  ester cellulose membrane (Millipore, Ireland) under vacuum. The resulting OPH/COOH-MWNTs paper (the filtration bed) was thoroughly rinsed with PBS and NaCl (1 M) to remove unreacted moieties.

OPH content in the resulting OPH/COOH-MWNTs papers was determined by measuring residual OPH concentration in the filtrate following fabrication. Thus, absorbance measurements were carried out at 280 nm using a microplate reader (Varioskan Flash, Thermo Scientific, USA).

## 2.6 Electron Microscopy

The nanostructure of the OPH/COOH-MWNTs conjugates (while dispersed) was investigated by cryogenic transmission electron microscopy (cryo-TEM). A small droplet of the OPH/COOH-MWNTs dispersion was placed on a perforated carbon film supported on a TEM copper grid (Ted Pella, Inc., USA), held by tweezers. It was then blotted by a piece of filter paper, resulting in the formation of thin films (100-300 nm) within the micropores of the grid. The specimen was then plunged into a reservoir of liquid ethane, cooled by liquid nitrogen, to ensure its vitrification and to prevent ice crystals formation. The vitrified specimen was transferred under liquid nitrogen and mounted on a cryogenic sample holder, cooled to  $-170^\circ\text{C}$ . Vitrified samples were examined in a FEI T12 G2 Cryo-TEM, operating at 120 kV, using a Gatan 626 cryo-holder. Images were recorded in a Gatan US1000 high-resolution cooled CCD camera and were processed with DigitalMicrograph software version 3.3.1. The ramp-shaped optical density gradients in the background were digitally corrected.

The morphology of OPH/COOH-MWNTs papers was characterized using a LEO 982 (Cambridge, UK) high resolution scanning electron microscopy (HRSEM), equipped with a high-resolution field emission gun (FEG), operating at a 4 kV accelerating voltage, a working distance of 3-4 mm, and an in-lens detector of secondary electrons.

## 2.7 FTIR spectroscopy

Attenuated total reflectance Fourier transform infrared (ATR-FTIR) spectroscopy spectra of the OPH/COOH-MWNTs membranes were recorded using a Thermo 6700 FT-IR equipped with a Smart iTR diamond ATR device.

## 2.8 Specific surface area measurements

The specific surface area of the OPH/COOH-MWNTs membranes was measured using a single-point BET on a Monosorb II analyzer (QuantaChrom).

## 2.9 Enzymatic hydrolysis of methyl paraoxon by OPH/COOH-MWNT papers

A volume of 5 mL of MOX (1.5 mM) aqueous solution in CHES is poured onto the OPH/COOH-MWNTs paper and vacuum filtered. The degree of MOX hydrolysis was determined by quantifying the concentration of the degradation product, p-nitrophenol, in the filtrate, as previously described. Note that the p-nitrophenol concentration was measured at the end of each filtration cycle i.e. after  $\sim 1$  h. The obtained filtrate solution was retreated by subsequent filtration steps using the same OPH/COOH-MWNTs membrane and p-nitrophenol concentration is measured in the filtrate after each cycle.

## 3. Results and discussion

### 3.1 Conjugation of OPH to CNTs

The synthesis scheme for the conjugation of the OPH enzyme to CNTs is outlined in Figure 1a. Prior to the enzyme attachment, two types of oxidized MWNTs were synthesized according to a known oxidative wet-chemistry method<sup>26, 47, 48</sup> using a mixture solution of concentrated  $\text{HNO}_3$  and  $\text{H}_2\text{SO}_4$ , towards corresponding carboxylic acid-functionalized multi-walled CNTs (COOH-MWNTs). These COOH-MWNTs as well as commercially available carboxylated MWNTs and double-walled CNTs are exfoliated in an aqueous surfactant (Triton-X 100) solution by ultrasonication to yield highly-dispersed CNTs suspensions<sup>49</sup>. Subsequently, direct coupling of OPH to the carboxylic acid functionalized CNTs is performed after their activation with N-hydroxysuccinimide (NHS) using 1-Ethyl-3-(3-dimethylaminopropyl) carbodiimide hydrochloride (EDC) coupling chemistry<sup>30, 50, 51</sup>. OPH conjugation in highly dispersed CNTs suspensions increase enzyme immobilization owing to the greater interfacial volume for interaction between the OPH and COOH-CNTs<sup>30</sup>. The reaction is followed by intensive centrifugation and rinsing to remove unreacted species.

The enzymatic activity of the different OPH-CNTs conjugates is characterized by measuring the hydrolysis rate of methyl paraoxon (MOX), used as a model OP substrate. The catalytic hydrolysis of MOX produces equimoles of p-nitrophenol, and its formation is determined spectrophotometrically. Figure 1b depicts the enzymatic activity of the different OPH-CNTs conjugates, normalized with respect to the CNTs mass, as a function of the hydrolysis reaction time. The highest OPH activity is observed for conjugates in which carboxylic acid-functionalized MWNTs (Nanocyl) fabricated in our laboratory have been used. After approximately two hours, this conjugate exhibits an enzymatic activity that is at least 50% higher in comparison to all other conjugates. It should be noted that conjugates based on the 'in-house' oxidized MWNTs outperform those prepared from commercially available carboxylated CNTs. This is ascribed to the higher content of carboxylic acid groups on the CNTs surface, resulting in higher protein conjugation efficiency<sup>52</sup>. Thus, based on these catalytic activity results, the COOH-MWNTs (Nanocyl) system has been further used in this work.

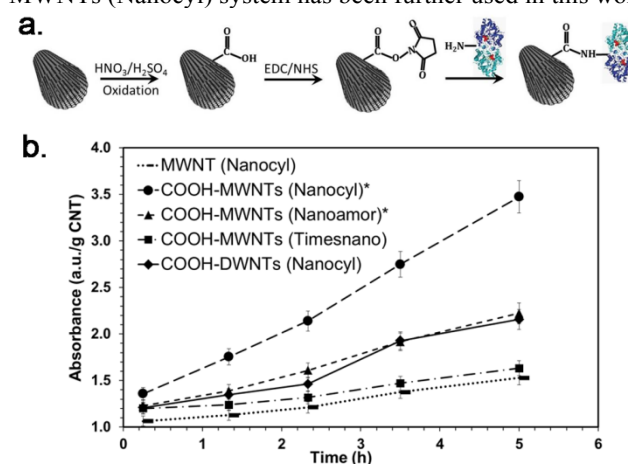


**Fig 1** (a) Synthesis scheme for the covalent immobilization of OPH to COOH-CNTs, (b) Enzymatic activity of the different OPH/COOH-

## ARTICLE

CNTs conjugates, normalized with respect to the CNTs mass, vs. hydrolysis reaction time.

### 3.2 Fabrication of OPH/COOH-MWNT papers

The next step is to develop CNTs papers that exhibit a biocatalytic activity, and can be potentially applied as a thin bioreactor for OPs bioremediation processes. We envisaged two possible methods for fabricating such membranes. The first and straightforward approach would be to pre-synthesize the CNT-enzyme conjugates followed by their dispersion and subsequent microfiltration, to yield a freestanding paper. The main drawback of this route is the essential re-dispersion step, which involves harsh ultrasonication conditions of the CNT-enzyme conjugates. Despite the widespread use of ultrasonication in various research disciplines and industries, the effects of ultrasonic energy on the stability and function of enzymes is not well characterized<sup>53</sup>. Ultrasonication has been shown to affect the secondary structure of enzymes, disrupting the active site conformation<sup>53</sup>, which in turn may result in the loss of enzymatic activity<sup>54</sup>. In addition, the multiple steps and time-consuming separation processes also present a significant disadvantage. Thus, an alternative and more attractive approach would be to carry out the enzyme conjugation reaction simultaneously to membrane formation. This 'one-pot' method may allow for a rapid and facile route for the fabrication of enzymatically-active CNT papers. The following sections will describe the bioactive paper synthesis and assembly by this methodology.

The first step is to disperse the COOH-CNTs in an aqueous surfactant solution by ultrasonication. The next step involves a microfiltration process, to generate the porous membrane, commonly termed buckypaper, assembled from entangled nanotubes. Herein, OPH conjugation to the COOH-CNTs is carried out during the microfiltration process. The EDC cross-linker is added to the filtered nanotubes dispersion, to activate the carboxylic acid groups and allow *in situ* conjugation to the OPH primary amines *via* amide bonds. The resulting membrane is thoroughly rinsed with NaCl solution (1 M) to remove unreacted species and in particular the non-covalently attached enzyme.

In order to confirm the immobilization of the OPH onto the nanotubes, the dispersion is sampled during the microfiltration process followed by ultra-fast cooling vitrification<sup>55, 56</sup>. Cryo-transmission electron microscopy (cryo-TEM) imaging of the vitrified dispersion is presented in Figure 2. The nanotubes are observed to be individually dispersed within the aqueous solution, while the enzyme densely decorates their surface (Fig. 2a). Cryo-TEM images of neat COOH-MWNTs dispersions (Fig. 2b) and corresponding OPH/COOH-MWNTs dispersions, in which the coupling agent EDC is omitted (Fig. 2c), clearly show that the native nanotube surface is smooth. In the case of the OPH/COOH-MWNTs system, minor protein adsorption to the nanotubes surface can be observed. These results are ascribed to nonspecific adsorption of the OPH enzyme onto the nanotube surface, as previously demonstrated<sup>57-59</sup>. Thus, cryo-TEM studies reveal the successful covalent immobilization of OPH onto MWNTs by the aforementioned 'one-pot' process.

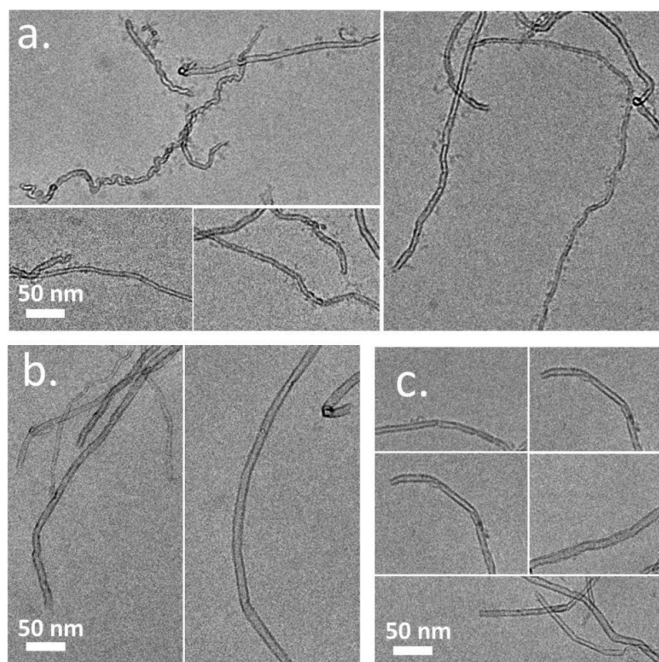


**Fig. 2** Cryo-TEM images of: (a) OPH/COOH-MWNTs dispersion. The MWNTs are observed to be individually dispersed within the aqueous solution, while the OPH densely decorates the nanotube surface. (b) OPH/COOH-MWNTs dispersion, in which the coupling agent EDC is omitted and (c) neat COOH-MWNTs dispersion (no enzyme).

Figure 3a shows an image of a typical freestanding OPH/COOH-MWNTs paper (thickness of  $\sim 100 \mu\text{m}$  and diameter of 16 mm), prepared via the 'one-pot' process, demonstrating its integrity and mechanical stability. The morphology of the resulting paper is investigated by high-resolution scanning electron microscopy (HRSEM) and compared to that of a neat COOH-MWNTs (no OPH) paper, see Figure 3b and c, respectively. Both membranes exhibit a porous nanostructure of highly entangled MWNTs, typical of buckypaper<sup>32-34, 60-66</sup>, with pores size in the range of 20-150 nm. The interconnected CNT network nanostructure allows obtaining a significant surface area of  $275 \pm 25 \text{ m}^2/\text{g}$ , determined by nitrogen adsorption and BET analysis. The fine OPH decoration, observed by cryo-TEM, cannot be detected by HRSEM for the OPH/CNTs membranes, possibly due to the lack of sufficient contrast and resolution. In addition, entrapped enzyme aggregates, within the porous MWNTs network, cannot be distinguished. Thus, HRSEM studies demonstrate that enzyme immobilization does not alter the porous paper structure.

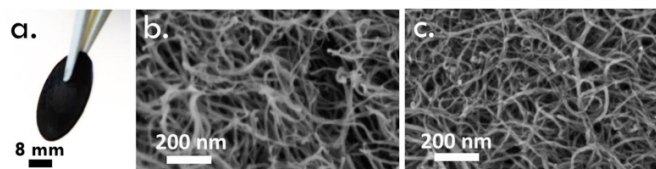


**Fig 3** (a) Image of a typical freestanding OPH/COOH-MWNTs paper prepared *via* the 'one-pot' process, (b) high-resolution SEM micrographs of OPH/COOH-MWNTs and (c) neat COOH-MWNTs (no OPH) papers. Both systems exhibit a porous nanostructure of highly entangled MWNTs

Attenuated total reflectance Fourier transform infrared (ATR-FTIR) spectroscopy of the OPH/COOH-MWNTs paper is employed as a complementary tool for confirming

immobilization of OPH onto the carboxylated nanotubes. Figure 4 depicts the ATR-FTIR spectra of the OPH/COOH-MWNTs paper and the corresponding neat COOH-MWNTs system. The OPH/COOH-MWNTs paper exhibits typical absorbance bands for both the  $\alpha$ -helix and  $\beta$ -sheet conformations of the enzyme.<sup>22</sup> The frequency peaks at 1658, 1644, 1557, and 1537  $\text{cm}^{-1}$  correspond to the  $\alpha$ -helix and those at 1694, 1682, 1633, and 1620  $\text{cm}^{-1}$  correspond to the  $\beta$ -sheet conformations.<sup>22, 30</sup> These bands are not observed for the COOH-MWNTs membranes.<sup>30</sup> Thus, ATR-FTIR spectroscopy confirms the enzyme immobilization within the CNT network. Bands ascribed to specific amide bonds between the OPH and the COOH-MWNTs cannot be detected. Nevertheless, it should be emphasized that the OPH/COOH-MWNTs papers are rigorously rinsed with NaCl solution in order to remove any physisorbed moieties. Namely, we assume that the characteristic OPH bands, observed for the OPH/COOH-MWNTs paper, can be assigned to the covalently attached enzyme.<sup>22, 30</sup> Based on this assumption, we calculate the immobilization reaction yield to be 44% (determined by measuring residual OPH concentration in the filtrate following paper fabrication). Thus, the enzyme loading in the resulting OPH/COOH-MWNTs paper is 862 mg/g (expressed as mg OPH per gram MWNTs), which is one order of magnitude higher in comparison to previously reported studies, in which OPH was immobilized onto polyurethane scaffolds and silica particles.<sup>24, 25</sup>

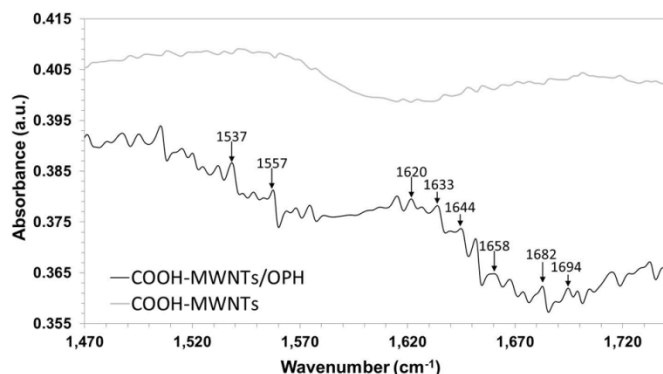


Fig. 4 ATR-FTIR spectra of OPH/COOH-MWNTs and neat COOH-MWNTs papers.

### 3.2 Enzymatic hydrolysis of methyl paraoxon by OPH/COOH-MWNT papers

Previous sections have demonstrated that our new “one-pot” synthetic approach results in a CNT paper, in which the OPH enzyme is covalently immobilized onto nanotubes surface. Figure 5 schematically illustrates the structure of the resulting membranes. To investigate the potential of this platform for bioremediation processes, we have studied the effect of filtering a model OP (MOX) solution through the membrane. It is well established that the OPH enzyme hydrolyze, and thereby detoxify, a broad range of OPs.<sup>67</sup> Enzymatic hydrolysis of common OPs reduces their toxicity by nearly 120-fold.<sup>68</sup> Moreover, it was shown that enzymatic hydrolysis is 450 times faster in comparison to conventional chemical hydrolysis processes (e.g., by 0.1 N sodium hydroxide)<sup>69</sup>.

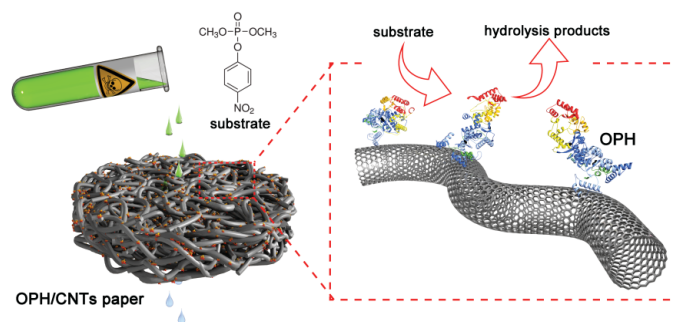


Fig. 5 Schematic illustration of the structure and the functionality of the biocatalytic OPH/COOH-MWNTs paper. A model OP (MOX) solution is filtered through the paper-like membrane and a decrease in MOX concentration is obtained due to its *in situ* hydrolysis by the immobilized OPH during the filtration process.

An aqueous solution of 1.5 mM MOX (5 mL) is poured onto the OPH/COOH-MWNTs paper and vacuum filtered. This MOX concentration is used in order to simulate a highly contaminated OPs solution. For example, according to European Union regulations, a permitted concentration of OPs in groundwater is  $0.1 \mu\text{g l}^{-1}$ .<sup>70</sup> The degree of MOX hydrolysis is determined by quantifying the concentration of the degradation product, p-nitrophenol, in the filtrate. The p-nitrophenol concentration was measured at the end of the filtration i.e. after  $\sim 1$  h. The obtained filtrate solution is retreated by subsequent filtration steps using the same OPH/COOH-MWNTs membrane. The calculated MOX concentration after each filtration cycle depicted in Figure 6. MOX concentration decreases by more than 10% following the first filtration cycle. Considering the low residence time in the membrane, as dictated by the paper’s dimensions (100  $\mu\text{m}$  thick), reduction in MOX content is relatively significant. This point will be discussed in detail in the following sections.

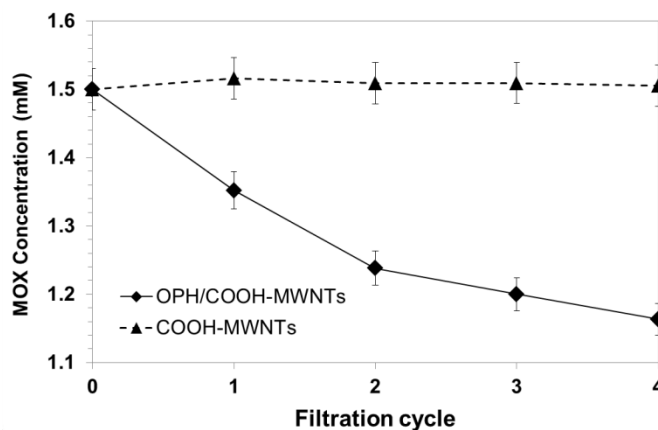


Fig. 6 Methyl paraoxon (MOX) concentration vs. the number of treatment/filtration cycles using the same OPH/COOH-MWNTs paper.

To verify that the reduction in MOX concentration is ascribed to its enzymatic hydrolysis, the filtration processes is also performed by using a neat COOH-MWNTs paper (no enzyme). Indeed, in this case, MOX concentration is unchanged (see Fig. 6). These experiments confirm that the decrease in MOX content results from its *in situ* hydrolysis by the immobilized OPH during the microfiltration process. Thus, the resulting enzymatically-active paper presents a facile bioremediation route to treat OPs contaminations. By carrying out subsequent treatment cycles it is possible to further reduce MOX content as

shown in Figure 6. This result demonstrates that the OPH/COOH-MWNTs paper maintains its functionality throughout the entire experiment (4 cycles). Additionally, reuse of the paper after several days results in similar MOX biodegradation efficiency (data not shown). Thus, these results confirm that the paper preserves its catalytic performance and demonstrates that this 'one-pot' fabrication route results in robust scaffolds for OP's bioremediation.

The OPH/COOH-MWNTs paper can be considered as a thin membrane bioreactor in analogy to conventional fibrous-bed bioreactors<sup>71</sup>. Important characteristics of the system *i.e.*, porosity, residence time and enzyme loading are calculated. The porosity (voids fraction) of the membrane ( $\epsilon$ ) is calculated according to following equation:

$$\epsilon = \frac{V_{total} - \frac{d_{MWNT} S_{total}}{4}}{V_{total}} \quad (1)$$

where  $V_{total}$  is the volume of the membrane according to its dimensions,  $S_{total}$  is the membrane surface area as measured by BET and  $d_{MWNT}$  is the average diameter of a single MWNT. The calculated porosity value is  $0.72 \pm 0.1$ . This high porosity value is within the range of typical buckypaper systems reported in the literature<sup>72</sup>.

The residence time, defined as the ratio between the voids volume and the volumetric flow rate, is calculated to be  $10.4 \pm 1.5$  s. It is important to note that the residence time in the OPH/COOH-MWNTs membrane is at least one order of magnitude lower in comparison to conventional OPH-based packed-bed bioreactors previously reported<sup>19, 73</sup>. Thus, considering the low residence time in the studied system, the achieved MOX biodegradation is significant (22%). Hence, for practical applications, the system should be further optimized in terms of the residence time (*e.g.*, by increasing the membrane thickness) in order to achieve higher hydrolysis efficiencies.

#### 4. Conclusion

Different OPH-CNTs conjugates have been prepared and their enzymatic activity was determined. Based on these results, a specific 'in-house' synthesized carboxylated-MWNTs system was identified to exhibit superior catalytic activity when conjugated with the OPH enzyme, and was therefore further used in this work. A new 'one-pot' methodology for *in situ* immobilization of OPH onto CNTs surface was developed. It should be emphasized that the covalent attachment of the OPH occurs simultaneously to the CNTs paper formation, and their enzymatic activity is confirmed. Thus, this generic process allows for a rapid and facile construction of enzymatically-active nanostructured scaffolds. To demonstrate the potential of the OPH/COOH-MWNTs papers for bioremediation, we have studied the effect of treating a model OP (MOX) solution with these miniaturized membranes. Indeed, significant decrease in MOX concentration is obtained, which is ascribed to *in situ* hydrolysis of MOX by the immobilized OPH during the filtration process. The unique combination of the high enzyme loading in these CNT membranes together with their high mechanical integrity allows for construction and miniaturization of conventional bio-catalytic systems *e.g.*, packed-bed bioreactors. This proof-of-concept study presents a new approach for the design of bioactive nano-scaffolds, which can be rationally tailored for a variety of applications ranging from environmental remediation to biomedical devices.

#### Acknowledgements

The authors thank M. Narkis for helpful discussions and continuous support. The Russell Berrie Nanotechnology Institute is gratefully acknowledged for supporting this research. We thank E. Kessleman and Y. Talmon for their help with cryo-TEM studies.

#### Notes and references

<sup>a</sup>Department of Chemical Engineering, Technion – Israel Institute of Technology, Haifa 32000, Israel.

<sup>b</sup>Department of Biotechnology and Food Engineering, Technion – Israel Institute of Technology, Haifa 32000, Israel.

<sup>c</sup>Department of Chemistry, Nanomaterials Research Center, Institute of Nanotechnology and Advanced Materials, Bar-Ilan University, Ramat-Gan 52900, Israel

<sup>†</sup>The Russell Berrie Nanotechnology Institute, Technion – Israel Institute of Technology, Haifa 32000, Israel

- H. F. Jia, G. Y. Zhu and P. Wang, *Biotechnology and Bioengineering*, 2003, **84**, 406-414.
- L. Wang, L. Wei, Y. Chen and R. Jiang, *Journal of Biotechnology*, 2010, **150**, 57-63.
- J. Bajgar, *Acta Medica (Hradec Kralove, Czech Republic)*, 2005, **48**, 3-21.
- J. Wu, C. Lan and G. Y. S. Chan, *Chemosphere*, 2009, **76**, 1308-1314.
- N. Saifuddin, A. Z. Raziah and A. R. Junizah, *Journal of Chemistry*, 2013.
- A. Mulchandani, W. Chen, P. Mulchandani, J. Wang and K. R. Rogers, *Biosensors & Bioelectronics*, 2001, **16**, 225-230.
- Q. Zhang and S. O. Pehkonen, *Journal of Agricultural and Food Chemistry*, 1999, **47**, 1760-1766.
- Q. Wang and A. T. Lemley, *Water Research*, 2002, **36**, 3237-3244.
- H. Shemer and K. G. Linden, *Journal of Hazardous Materials*, 2006, **138**, 638.
- K. A. Mohamed, A. A. Basfar, H. A. Al-Kahtani and K. S. Al-Hamad, *Radiation Physics and Chemistry*, 2009, **78**, 994-1000.
- J.-J. Yu, *Water Research*, 2002, **36**, 1095-1101.
- K. Y. Foo and B. H. Hameed, *Journal of Hazardous Materials*, 2010, **175**, 1-11.
- E. S. K. Chian, W. N. Bruce and H. H. P. Fang, *Environmental Science and Technology*, 1975, **9**, 52-59.
- S.-S. Chen, J. S. Taylor, L. A. Mulford and C. D. Norris, *Desalination*, 2004, **160**, 103-111.
- Y. Kiso, Y. Sugiura, T. Kitao and K. Nishimura, *Journal of Membrane Science*, 2001, **192**, 1-10.
- G. Aragay, F. Pino and A. Merkoci, *Chemical Reviews*, 2012, **112**, 5317-5338.
- J. Cabal, J. Micova and K. Kuca, *Journal of Applied Biomedicine*, 2010, **8**, 111-116.
- J. K. Raynes, F. G. Pearce, S. J. Meade and J. A. Gerrard, *Biotechnology Progress*, 2011, **27**, 360-367.
- A. A. Wang, W. Chen and A. Mulchandani, *Biotechnology and Bioengineering*, 2005, **91**, 379-386.
- A. J. Ghoshdastidar, J. E. Saunders, K. H. Brown and A. Z. Tong, *Journal of Environmental Science and Health, Part B: Pesticides, Food Contaminants, and Agricultural Wastes*, 2012, **47**, 742-750.

21. J. P. Walker, K. W. Kimble and S. A. Asher, *Analytical and Bioanalytical Chemistry*, 2007, **389**, 2115-2124.
22. J. Orbulescu, C. A. Constantine, V. K. Rastogi, S. S. Shah, J. J. DeFrank and R. M. Leblanc, *Analytical Chemistry*, 2006, **78**, 7016-7021.
23. A. Mulchandani, P. Mulchandani, I. Kaneva and W. Chen, *Analytical Chemistry*, 1998, **70**, 4140-4145.
24. A. K. Singh, A. W. Flounders, J. V. Volponi, C. S. Ashley, K. Wally and J. S. Schoeniger, *Biosensors & Bioelectronics*, 1999, **14**, 703-713.
25. P. L. Havens and H. F. Rase, *Industrial & Engineering Chemistry Research*, 1993, **32**, 2254-2258.
26. S. R. Caldwell and F. M. Raushel, *Applied Biochemistry and Biotechnology*, 1991, **31**, 59-73.
27. W. Feng and P. Ji, *Biotechnology Advances*, 2011, **29**, 889-895.
28. R. P. Deo, J. Wang, I. Block, A. Mulchandani, K. A. Joshi, M. Trojanowicz, F. Scholz, W. Chen and Y. H. Lin, *Analytica Chimica Acta*, 2005, **530**, 185-189.
29. D. Du, W. Chen, W. Zhang, D. Liu, H. Li and Y. Lin, *Biosensors & Bioelectronics*, 2010, **25**, 1370-1375.
30. V. A. Pedrosa, S. Paliwal, S. Balasubramanian, D. Nepal, V. Davis, J. Wild, E. Ramanculov and A. Simonian, *Colloids and Surfaces B-Biointerfaces*, 2010, **77**, 69-74.
31. M. Trojanowicz, *Trac-Trends in Analytical Chemistry*, 2006, **25**, 480-489.
32. I. W. P. Chen, Z. Liang, B. Wang and C. Zhang, *Carbon*, 2010, **48**, 1064-1069.
33. S. M. Cooper, H. F. Chuang, M. Cinke, B. A. Cruden and M. Meyyappan, *Nano Letters*, 2003, **3**, 189-192.
34. X. Fu, C. Zhang, T. Liu, R. Liang and B. Wang, *Nanotechnology*, 2010, **21**.
35. B. J. Hinds, N. Chopra, T. Rantell, R. Andrews, V. Gavalas and L. G. Bachas, *Science (Washington, DC, United States)*, 2004, **303**, 62-65.
36. I. Kang, M. J. Schulz, J. H. Kim, V. Shanov and D. Shi, *Smart Materials and Structures*, 2006, **15**, 737-748.
37. M. Pacios, M. del Valle, J. Bartroli and M. J. Esplandiú, *Journal of Electroanalytical Chemistry*, 2008, **619-620**, 117-124.
38. G. Whitten Philip, A. Gestos Adrian, M. Spinks Geoffrey, J. Gilmore Kerry and G. Wallace Gordon, *Journal of biomedical materials research. Part B, Applied biomaterials*, 2007, **82**, 37-43.
39. L. Halamkova, J. Halamek, V. Bocharova, A. Szczupak, L. Alfonta and E. Katz, *J. Am. Chem. Soc.*, 2012, **134**, 5040-5043.
40. M. Southcott, K. MacVittie, J. Halamek, L. Halamkova, W. D. Jemison, R. Lobel and E. Katz, *Phys. Chem. Chem. Phys.*, 2013, **15**, 6278-6283.
41. A. Szczupak, J. Halamek, L. Halamkova, V. Bocharova, L. Alfonta and E. Katz, *Energy Environ. Sci.*, 2012, **5**, 8891-8895.
42. S. Chatterjee and A. Chen, *Biosensors & Bioelectronics*, 2012, **35**, 302-307.
43. K. Sears, L. Dumeé, J. Schutz, M. She, C. Huynh, S. Hawkins, M. Duke and S. Gray, *Materials*, 2010, **3**, 127-149.
44. A. S. Brady-Estevéz, M. H. Schnoor, S. Kang and M. Elimelech, *Langmuir*, 2010, **26**, 19153-19158.
45. H. Y. Yang, Z. J. Han, S. F. Yu, K. L. Pey, K. Ostrikov and R. Karnik, *Nature communications*, 2013, **4**, 2220-2220.
46. L. F. Dumeé, K. Sears, J. Schuetz, N. Finn, C. Huynh, S. Hawkins, M. Duke and S. Gray, *Journal of Membrane Science*, 2010, **351**, 36-43.
47. D. Goldman and J.-P. Lellouche, *Carbon*, 2010, **48**, 4170-4177.
48. M. Piran, V. Kotlyar, D. D. Medina, C. Pirlot, D. Goldman and J.-P. Lellouche, *J. Mater. Chem.*, 2009, **19**, 631-638.
49. G. Mechrez, R. Y. Suckeveriene, R. Tchoudakov, A. Kigly, E. Segal and M. Narkis, *J. Mater. Sci.*, 2012, **47**, 6131-6140.
50. W. Yang, P. Thordarson, J. J. Gooding, S. P. Ringer and F. Braet, *Nanotechnology*, 2007, **18**, 412001/412001-412001/412012.
51. R. Pauliukaite, M. E. Ghica, O. Fatibello-Filho and C. M. A. Brett, *Anal. Chem. (Washington, DC, U. S.)*, 2009, **81**, 5364-5372.
52. K. Y. Jiang, L. S. Schadler, R. W. Siegel, X. J. Zhang, H. F. Zhang and M. Terrones, *Journal of Materials Chemistry*, 2004, **14**, 37-39.
53. A. Guiseppi-Elie, S.-H. Choi and K. E. Geckeler, *J. Mol. Catal. B: Enzym.*, 2009, **58**, 118-123.
54. S. Shah and M. N. Gupta, *Chemistry Central Journal*, 2008, **2**.
55. Y. Talmon, *Surfactant Science Series*, 1999, **83**, 147-178.
56. C. J. Newcomb, T. J. Moyer, S. S. Lee and S. I. Stupp, *Current Opinion in Colloid & Interface Science*, 2012, **17**, 350-359.
57. N. Liu, X. Cai, Y. Lei, Q. Zhang, M. B. Chan-Park, C. Li, W. Chen and A. Mulchandani, *Electroanalysis*, 2007, **19**, 616-619.
58. S. S. Karajanagi, A. A. Vertegel, R. S. Kane and J. S. Dordick, *Langmuir*, 2004, **20**, 11594-11599.
59. T.-W. Tsai, G. Heckert, L. F. Neves, Y. Tan, D.-Y. Kao, R. G. Harrison, D. E. Resasco and D. W. Schmidtke, *Analytical Chemistry*, 2009, **81**, 7917-7925.
60. W. Zhu, D. Ku, J. P. Zheng, Z. Liang, B. Wang, C. Zhang, S. Walsh, G. Au and E. J. Plichta, *Electrochimica Acta*, 2010, **55**, 2555-2560.
61. J. G. Park, S. Li, R. Liang, C. Zhang and B. Wang, *Carbon*, 2008, **46**, 1175-1183.
62. R. L. D. Whitby, T. Fukuda, T. Maekawa, S. L. James and S. V. Mikhailovsky, *Carbon*, 2008, **46**, 949-956.
63. M. Endo, H. Muramatsu, T. Hayashi, Y. A. Kim, M. Terrones and N. S. Dresselhaus, *Nature*, 2005, **433**, 476-476.
64. E. D. Laird, W. Wang, S. Cheng, B. Li, V. Presser, B. Dyatkin, Y. Gogotsi and C. Y. Li, *ACS Nano*, 2012, **6**, 1204-1213.
65. D. Simien, J. A. Fagan, W. Luo, J. F. Douglas, K. Migler and J. Obrzut, *ACS Nano*, 2008, **2**, 1879-1884.
66. A. N. Volkov and L. V. Zhigilei, *ACS Nano*, 2010, **4**, 6187-6195.
67. R. S. Makkar, A. A. DiNovo, C. Westwater and D. A. Schofield, *J. Biorem. Biodegrad.*, 2013, **4**, 1000182/1000181-1000182/1000187.
68. A. Singh, O. P. Ward and Editors, *Biodegradation and Bioremediation. [In: Soil Biol.; 2004, 2]*, Springer GmbH, 2004.
69. D. M. Munnecke, *Applied and Environmental Microbiology*, 1976, **32**, 7-13.
70. M. Diagne, N. Oturan and M. A. Oturan, *Chemosphere*, 2007, **66**, 841-848.
71. V. Nedovic, R. Willaert and Editors, *Fundamentals of Cell Immobilisation Biotechnology. [In: Focus Biotechnol.; 2004, 8A]*, Kluwer Academic Publishers, 2004.
72. A. Martinelli, G. A. Carru, L. D'Ilario, F. Caprioli, M. Chiaretti, F. Crisante, I. Francolini and A. Piozzi, *Acs Applied Materials & Interfaces*, 2013, **5**, 4340-4349.
73. A. H. Mansee, W. Chen and A. Mulchandani, *Journal of Industrial Microbiology & Biotechnology*, 2005, **32**, 554-560.